Journal of Alloys and Compounds 708 (2017) 84–92

Contents lists available at ScienceDirect

Journal of Alloys and Compounds

journal homepage: http://www.elsevier.com/locate/jalcom

High strain rate compression behavior of a heavily stabilized beta titanium alloy: Kink deformation and adiabatic shearing

Youping Zheng [1], Weidong Zeng*, Yubo Wang, Dadi Zhou, Xiongxiong Gao

State Key Laboratory of Solidification Processing, Northwestern Polytechnical University, Xi'an 710072, PR China

A R T I C L E I N F O

Article history:
Received 13 October 2016
Received in revised form
21 February 2017
Accepted 27 February 2017
Available online 28 February 2017

Keywords:
High strain rate
Kink deformation
Adiabatic shearing
Rotational dynamic recrystallization

A B S T R A C T

High strain rate compression deformations at $5 \times 10^3 s^{-1}$ of Ti-35V-15Cr-0.3Si-0.1C beta titanium alloy were conducted at variant temperatures from 20 °C to 800 °C on split-Hopkinson pressure bar system. It is found that the dynamic stress-strain curves at such a high strain rate contain hardening stages and softening stages. Different stages suggest different deformation mechanisms. In the hardening stages, kink deformation is uncommonly observed. The formation of kink bands is found to be responsible for the hardening effect. Adiabatic shearing began with the stress drops in the softening stages. From then on, the deformations localized in narrow regions, where adiabatic shearing bands (ASBs) formed at last. Dynamic recrystallization (DRX) occurred in the ASBs. The ultra-fine recrystallization grains with grain size of 0.28 μm, 0.35 μm, and 4.5 μm are observed in the ASBs formed at 400 °C, 600 °C and 800 °C respectively. It is really hard so far to measure the true shear strains and the true temperatures in the ASBs. In order to estimate the true shear strains in the ASBs, an original method basing on the definition of shear strain is proposed in this paper. Then a modified equation using the true shear strain rather than the empirical factor is employed to estimate the true temperatures in the ASBs. On such a base, the DRX in present ASBs is well explained in kinetics via the rotational dynamic recrystallization (RDR) mechanism.

1. Introduction

In the metallic materials servicing at high strain rate, adiabatic shearing often takes place in a narrow zone of highly localized deformation named adiabatic shear band (ASB). ASBs are generally observed in ballistic impacts, armor penetrations, explosive fragmentations and serrated continuous chips formed in the high speed cutting [1,2]. In general, the formation of ASBs has been noted as a form of failure mechanisms as well as a precursor to ductile fracture and will degrade the dynamic properties of alloys [2]. Thus the research on the adiabatic shearing during high strain rate deformation has great significance to the materials servicing in the severe conditions.

The research work of adiabatic shearing behavior in various alloys at high strain rate has been reported so far. Wu et al. and Zhang et al. studied the Johnson-Cook model at high strain rates using Ti-6Al-2Sn-2Zr-3Mo-1Cr-2Nb alloy and Ti-6.6Al-3.3Mo-1.8Zr-0.29Si alloy [1,3]. On the 2919A aluminum alloy plate impacted at 300 °C, Gao et al. observed the adiabatic shearing lines with the strain rate from $679 s^{-1}$ to $2500 s^{-1}$ and adiabatic shearing bands with the strain rate of $5610 s^{-1}$ or higher [4]. Hao et al. found that the failure mechanism of Ti-47Al-2Cr-2Nb alloy at the strain rate of $3500 s^{-1}$ transferred from brittle shearing failure to adiabatic shearing failure at 200 °C [5]. The microstructure evolution in ASBs was extensively researched as well. Xu et al. found the distortion-free nanograins due to dynamic recrystallization (DRX) in ASBs on single crystal Fe-15Cr-15Ni alloy deformed at the strain rate of $10^4 s^{-1}$ [6]. Meyers et al. proposed the rotational dynamic recrystallization (RDR) mechanism to explain DRX in ASBs [7]. This model was employed to explain the DRX in ASBs formed in different alloys at high strain rate [6–11].

Although uncommon, kink deformation has been considered as an important deformation mode, especially for the materials exhibiting strong plastic anisotropy, such as polymers [12], ceramics [13,14] and metallic materials with hcp crystals [15,16]. The

---

* Corresponding author. State Key Laboratory of Solidification Processing, Northwestern Polytechnical University, No. 127 Youyi Xilu, Xi'an 710072, PR China.
E-mail addresses: zhenguping@qq.com (Y. Zheng), zengwd@nwpu.edu.cn (W. Zeng).

[1] Postal address: State Key Laboratory of Solidification Processing, Northwestern Polytechnical University, No. 127 Youyi Xilu, Xi'an 710072, PR China.

http://dx.doi.org/10.1016/j.jallcom.2017.02.284

dislocation model was proposed to explain the kink deformation for single zinc crystal [17]. The principle of the dislocation model was the geometrically necessary dislocations (GNDs) introduced in a deformed grain [16,18]. The concept of GNDs could be explained with the crystal cantilever beam model. However, kink deformation is scarcely observed in metallic materials with bcc lattice structures.

Ti-35V-15Cr-0.3Si-0.1C (wt. %) alloy (here after Ti3515 alloy) is a typical heavily stabilized beta titanium alloy with excellent burning resistance. Burning-resistant titanium alloys are typically applied to aero-engine components including cast compressor components and vectored exhaust structures. These parts are usually subjected to the foreign object damage (FOD) at high temperatures and high strain rates, e.g. ingesting small particles when aircrafts taking off or landing. The impact velocities of the typically foreign objects with size in millimeter regime are 100–350 m/s [19]. In this paper, high strain rate compression deformations of Ti3515 alloy were conducted with the temperatures ranging from room temperature to high temperatures. The dynamic stress-strain curves are found to contain two stages. The evolution of deformation mechanism is researched. Kink bands and ASBs are observed on deformed samples. The DRX in the ASBs on sample deformed at different temperatures is discussed.

2. Experiments

2.1. Materials and experiment procedures

The Ti3515 alloy used in this paper was provided by Western Superconducting Technologies Co., Ltd. in cast condition. As shown in Fig. 1, this alloy consists of coarse β grains and the grain size of is approximately 1~3 mm. In addition, there are some obvious precipitates with lath shapes. The laths have been proved to be carbides by the component analysis through energy disperse spectroscopy (EDS) in our other work [20].

The cylindrical samples with diameter of 5 mm and height of 4 mm were cut from the Ti3515 alloy ingot by the method of wire-electrode cutting. A series of high speed compression tests were conducted on split-Hopkinson pressure bar (SHPB) system at the strain rate of $5 \times 10^3 s^{-1}$ with the initial temperature range of 20 °C (Room temperature), 200 °C, 400 °C, 600 °C and 800 °C respectively according to the service temperature of Ti3515 alloy. SHPB is a technique widely used in studying the dynamic behavior of materials at high strain-rates [13,21]. The details of SHPB will be presented in the next section. After the tests, the dynamic stress-strain curves obtained during the tests were analyzed. Then the end surfaces of samples were grinded, polished and etched for ~30s in the corrosive reagent with the volume ratio HF:HNO_3:H_2O of 1:3:5.

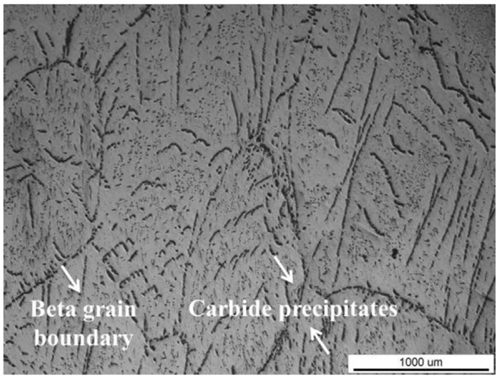

Fig. 1. Microstructures of as-received Ti3515 alloy.

Then the microstructures observation was conducted on an Olympus/GX71 optical microscope (OM) and a S4800 scanning electron microscope (SEM). The samples deformed at 800°C was subsequently electrolytic polished. EBSD analyses were employed on a JSM 6460 instrument equipped with an HKL Channel 5 system. The acceleration voltage was 20 kV and the tilting angle was 70°. Crystallographic orientation analyses were carried out using the EBSD results.

2.2. SHPB techniques

The Split-Hopkinson Pressure Bar (SHPB) system consists primarily of a strike bar, an incident bar and a transmission bar as shown in Fig. 2. Before the experiment, the cylindrical sample is usually sandwiched between the incident bar and the transmission bar. When a high-strain-rate compression test begins, the high pressure gas drives the strike bar to strike the incident bar. The strike produces a compressive elastic wave in the incident bar. The wave is partially reflected back at the interface between the incident bar and the sample. The rest of the wave transmits through the sample and the transmission bar (ignoring the reflected wave at the interface between the sample and the transmission bar). The reflected wave and transmitting wave are recorded by the strain gages installed on the incident bar and the transmission bar. Three equations are employed to calculate the flow stress σ, strain ε and strain rate $\dot{\varepsilon}$ as

$$\sigma = E\frac{A_b}{A_s}\varepsilon_t \tag{1}$$

$$\varepsilon = -2\frac{C}{L}\int \varepsilon_r dt \tag{2}$$

$$\dot{\varepsilon} = -2\frac{C}{L}\varepsilon_r \tag{3}$$

where ε_t and ε_r are the transmitting wave and the reflected wave respectively, A_b and A_s are the cross-sectional area of the bars and the sample, E and L are the Young's modulus and the gauge length of the sample, C is the traveling speed of the elastic wave in the bars and t is the time [13,21]. It is widely accepted that force equilibrium on the sample in SHPB test is established in the rising time duration t_r of the step signal of the incident wave pulse as shown in Fig. 3 [13,21]. So a maximum allowable sample length L_{max} is obtained as

$$L_{max} = \frac{1}{n}\frac{C_{SP}}{C}5r \approx \frac{5r}{n} \tag{4}$$

where C_{sp} is the traveling speed of the elastic wave in the sample, r is the radius of bars and n is the times stress waves travel along the length of the sample [21]. It is believed that the stress waves can

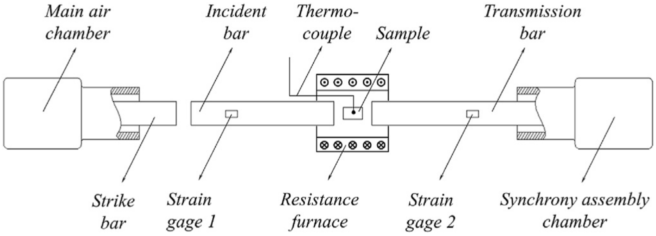

Fig. 2. Schematic of the SHPB system employed in present experiments containing a barrel type resistance furnace and a synchrony assembly subsystem.